

Highly Fluorescent, π -Extended Indenopyrido[2,1-*a*]isoindolone Derivatives Prepared by a Palladium-Catalysed Cascade Reaction

Zein el abidine Chamas,^[a] Enrico Marchi,^[b] Alberto Modelli,^[b] Yves Fort,^[a] Paola Ceroni,^{*[b]} and Victor Mamane^{*[a]}

Keywords: Cascade reactions / Polycycles / Nitrogen heterocycles / Chromophores / Fluorescence

A new family of heterocyclic pentacyclic compounds have been prepared by a cascade reaction involving 2,5-dihalo-pyridines and (2-formylphenyl)boronic acids. Most of the compounds exhibit high quantum yields of fluorescence in dichloromethane. In some cases, small changes in the substitution pattern caused fluorescence quenching. To rationalize

this effect, a detailed photophysical study combined with electrochemical and computational studies was performed on four representative derivatives. It appears that the fluorescence quenching is caused by a thermally activated non-radiative deactivation process that can be prevented in a rigid matrix such as ethanol at 77 K or a PMMA polymer.

Introduction

During the last few years, considerable attention has been devoted to the development of new organic fluorophores, as can be seen from the rising number of applications in materials science^[1] and biology.^[2] Of these fluorophores, nitrogen-containing, π -extended polycyclic systems based on the isoindole^[3] and indolizine^[4] frameworks are expected to exhibit excellent emitting properties. In particular, indolizino[3,4,5-*ab*]isoindoles prepared from pyrido[2,1-*b*]isoindoles have been found to be excellent fluorophores with high quantum yields and tuneable colours (Figure 1).^[5] Recently, other similar indolizine-based polyheterocyclic fluorescent dyes have been described that exhibit excellent photophysical properties.^[6] We recently reported the synthesis of indenopyrido[2,1-*a*]isoindolone derivatives, which constitute a new class of π -extended isoindolones possessing the same pyridoisoindole subunit^[7] as in indolizino[3,4,5-*ab*]isoindoles (Figure 1).^[8] These pentacyclic compounds were prepared by a palladium-catalysed cascade reaction starting from simple monocyclic 2,5-dihalo-pyridines and (2-formylphenyl)boronic acids.

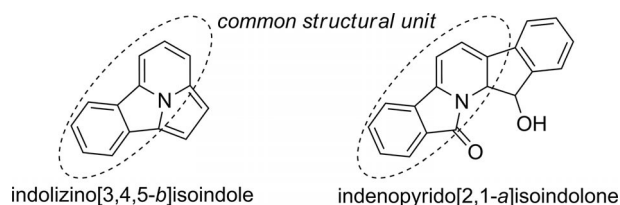


Figure 1. Fluorescent molecules with a pyridoisoindole subunit.

We report herein a large series of fluorescent pentacyclic compounds obtained by varying the substituents on the starting pyridine (4- and/or 6-positions) and/or the boronic acid (*meta* or *para* positions with respect to the boronic acid function, Figure 2). Because two boronic acids are involved in the reaction, sequential coupling of two different boronic acids allowed us to prepare the so-called “unsymmetrical” derivatives (different substitution of the A and C rings) in contrast to the “symmetrical” ones (same substitution of the A and C rings) obtained with two identical boronic acids. These pentacyclic compounds exhibit high fluorescence quantum yields in several cases, with the substitution pattern having a significant effect. The photophysical inves-

[a] Laboratoire SRSMC (UMR CNRS 7565), Université de Lorraine, BP 70239, Bd. des Aiguillettes, 54506 Vandoeuvre les Nancy, France
Fax: +33-3-83684785
E-mail: victor.mamane@univ-lorraine.fr
Homepage: <http://www.srsmc.uhp-nancy.fr/spip/>

[b] Department of Chemistry “G. Ciamician”, University of Bologna, Via Selmi 2, 40126 Bologna, Italy
E-mail: paola.ceroni@unibo.it
Homepage: <http://www.photonanoblab.com/>

Supporting information for this article is available on the WWW under <http://dx.doi.org/10.1002/ejoc.201201575>.

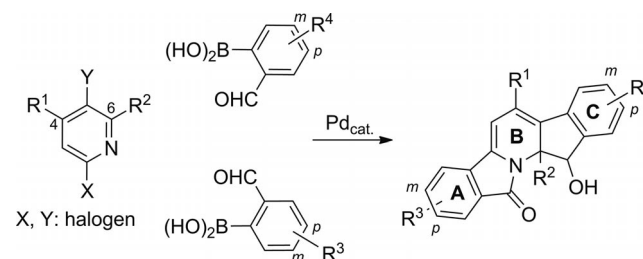


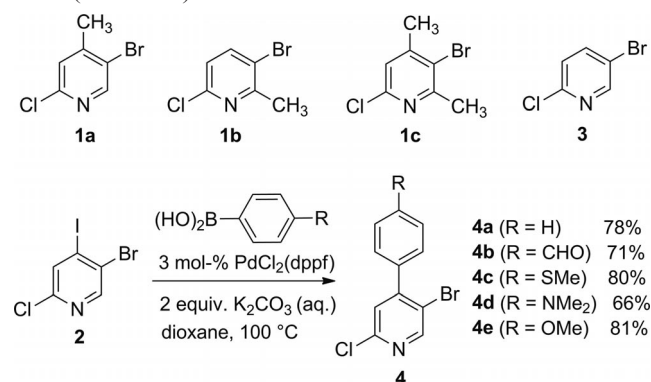
Figure 2. Functional group modification of the pentacyclic derivatives.

tigation was accompanied by electrochemical as well as computational studies.

Results and Discussion

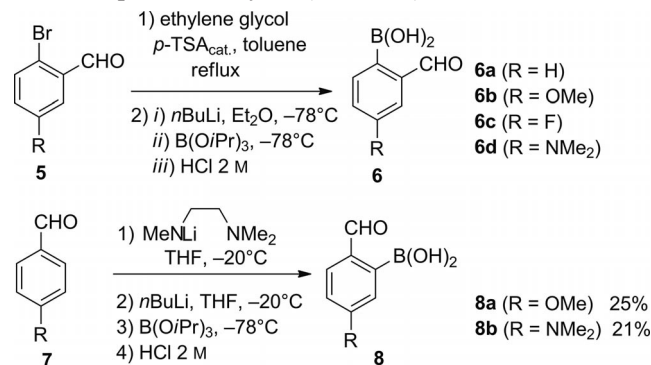
Synthesis of the Substituted Pyridines and Boronic Acids

5-Bromo-2-chloropyridines **1** bearing one or two methyl groups and trihalopyridine **2** were prepared according to literature procedures. The 4-substituted derivatives **1a** and **2**^[9] were obtained by an LDA-mediated lithiation of 5-bromo-2-chloropyridine (**3**) at -78°C ^[10] followed by electrophilic trapping whereas the 6-substituted compounds **1b** and **1c**^[8] were prepared from the corresponding 2-aminopyridines by a diazotization/substitution sequence. The trihalopyridine **2** was then used to prepare several 4-arylpyridines **4** by selective cross-coupling at C-4 bearing the iodine atom (Scheme 1).



Scheme 1. Pyridine substrates for the cascade reaction.

Boronic acids **6** with a substituent *para* to the B(OH)₂ group were prepared from the corresponding bromo derivatives **5** by known procedures.^[11] Boronic acids **8** containing a substituent *meta* to the B(OH)₂ group were prepared from the corresponding benzaldehydes **7** by using the Comins *ortho*-lithiation procedure^[12] and trapping with B(OiPr)₃. Despite the low yields obtained, this method allowed direct entry to rare and expensive (2-formylphenyl)boronic acids from cheap benzaldehydes (Scheme 2).



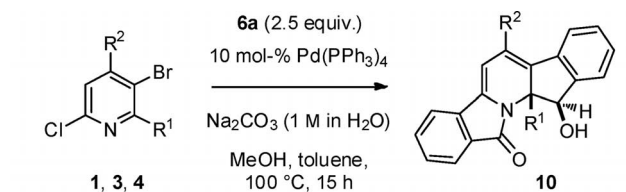
Scheme 2. Boronic acid substrates used in the cascade reaction.

Cascade Reaction

The “symmetrical” compounds were obtained by the reaction of 1 equiv. of the pyridine substrate with 2.5–3 equiv.

of the boronic acid. First, the effect of substituents on the pyridine was evaluated by treating pyridine **3** as well as all the 4- and/or 6-substituted 5-bromo-2-chloropyridines **1** and **4** with 2.5 equiv. of boronic acid **6a**. In all cases, the pentacyclic framework was formed and compounds **10** were isolated in moderate-to-good yields (Table 1).

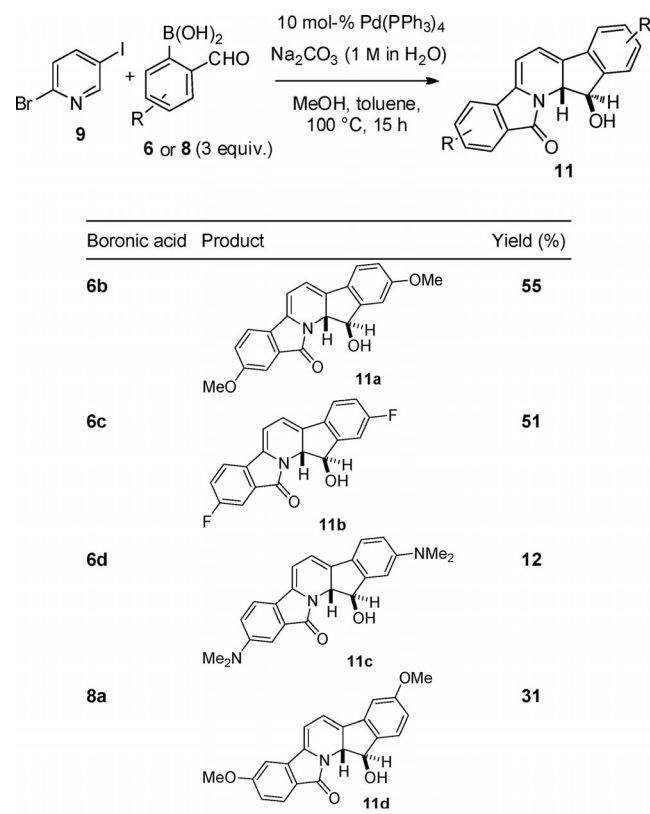
Table 1. Synthesis of “symmetrical” pentacyclic compounds by modification of the pyridine substrates.



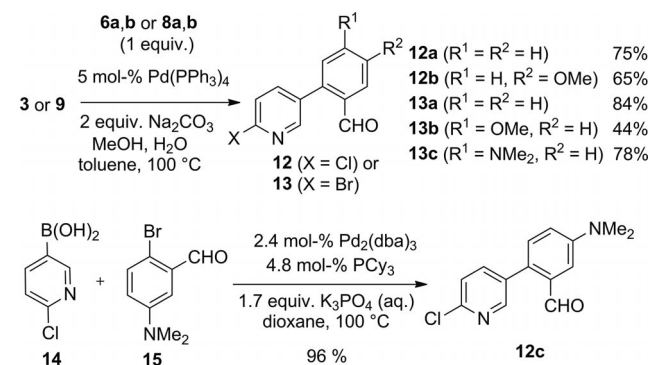
Pyridine	Product	Yield (%)	Pyridine	Product	Yield (%)
3	10a	57	4b	10f	70
1a	10b	50	4c	10g	37
1b	10c	59	4d	10h	46
1c	10d	36	4e	10i	56
4a	10e	60			

Differently substituted boronic acids **6** and **8** were also tested in the cascade process (Table 2). In these cases, the use of 2-bromo-5-iodopyridine (**9**) instead of **3** led to higher yields. The substituent on the boronic acid has a large influence on the yield of the reaction independently of its electronic nature. Thus, moderate-to-good yields of compounds **11a**, **11b** and **11d** were obtained with boronic acids **6b**, **6c** and **8a**, respectively, whereas compound **11c** was isolated in a poor yield of 12%.

Table 2. Synthesis of “symmetrical” pentacyclic compounds by modification of the boronic acid substrates.

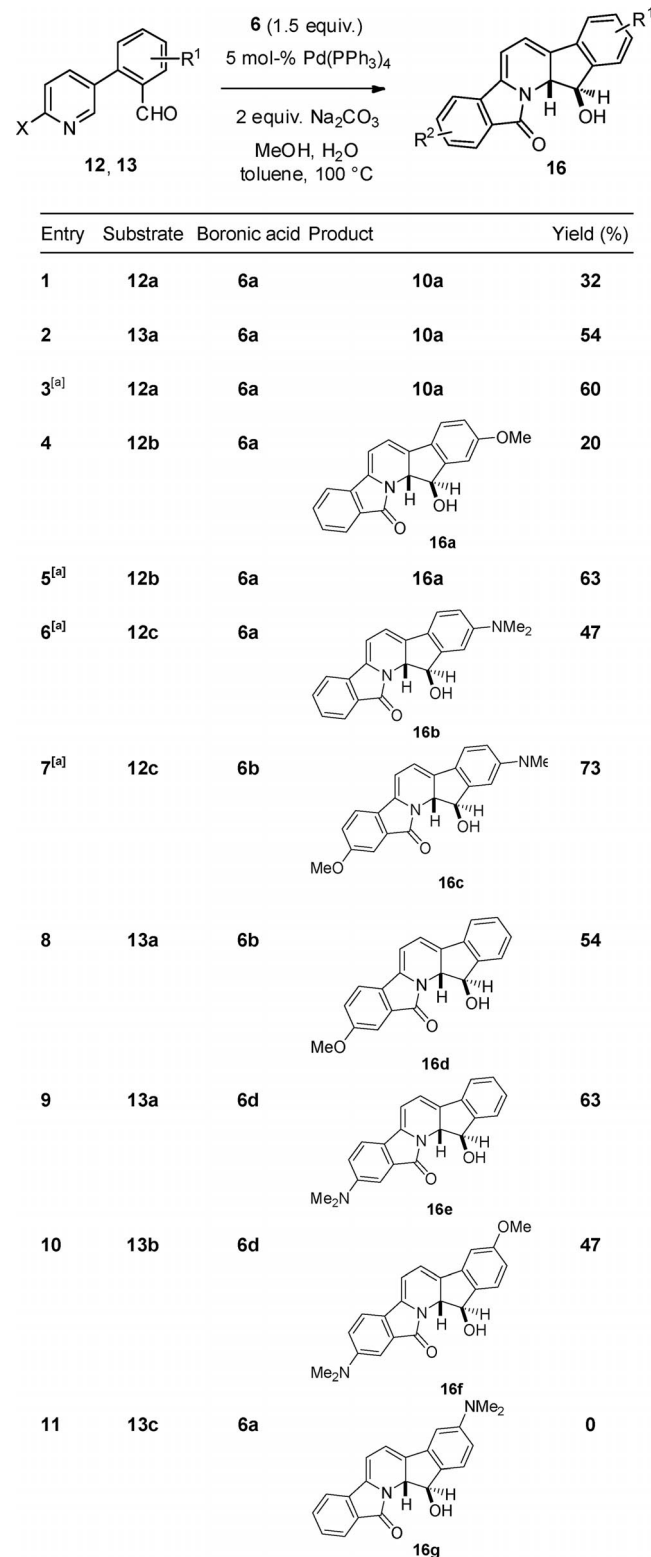


The “unsymmetrical” compounds were prepared by using a two-step procedure involving the isolation of the products after the first cross-coupling followed by the cascade reaction initiated by the second cross-coupling reaction. Several pyridylbenzaldehyde derivatives **12** and **13** bearing either a chlorine or bromine at the 2-position of the pyridine ring were prepared by coupling pyridines **3** and **9** with boronic acids **6a,b** and **8a,b** in the presence of $[\text{Pd}(\text{PPh}_3)_4]$ as catalyst. For **13c**, to increase the yield (relative to boronic acid **8b**), pyridine **9** was used in two-fold excess. These conditions were unsuccessful with boronic acid **6d** and therefore compound **12c** was synthesized by the



Scheme 3. Preparation of the pyridylbenzaldehyde substrates.

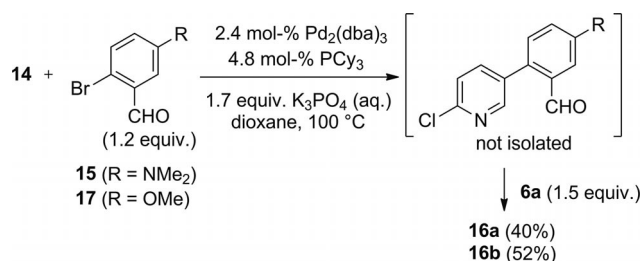
coupling of pyridylboronic acid **14** and bromobenzaldehyde **15** in an excellent yield of 96% by using the combination $[\text{Pd}_2(\text{dba})_3]/\text{PCy}_3$ as catalyst^[13] (Scheme 3).

Table 3. Synthesis of the “unsymmetrical” pentacyclic derivatives **16**.

[a] 1 equiv. of NaBr was added.

Derivatives **12** and **13** were then used in the cascade reaction with different boronic acids to obtain “unsymmetrical” compounds **16** (Table 3). First, **12a** and **13a** were treated with boronic acid **6a** to form **10a** in yields of 32 and 54%, respectively (entries 1 and 2). The yield of **10a** starting from **12a** could be increased to 60% by the addition of 1 equiv. of NaBr to the reaction mixture (entry 3). NaBr addition was also beneficial for the synthesis of **16a** from **12b** (compare entries 4 and 5). Therefore it was used in the cascade reactions involving substrate **12c** and boronic acids **6a** or **6b** to furnish **16b** and **16c**, respectively, in good yields (entries 6 and 7). Compounds **13a,b** reacted smoothly with boronic acids **6b** and **6d** under the standard conditions to give **16d–f** in good yields (entries 8–10), however, substrate **16g** was not isolated from the cascade reaction of **13c** with **6a** (entry 11).

We also explored the possibility of performing in a one-pot procedure the successive coupling of two differently substituted boronic acids without the isolation of the pyridylbenzaldehyde intermediates. Good yields of **16a,b** were obtained when boronic acid **14** was cross-coupled successively with bromobenzaldehydes **15** or **17** and then with **6a** by using the $[\text{Pd}_2(\text{dba})_3]/\text{PCy}_3$ catalytic system (Scheme 4). The use of boronic acid **14** has two advantages during the first step: It allows the formation of the intermediates in high yields and avoids the generation of over-coupling products enabling an easy isolation of the final cascade products **16a,b**.



Scheme 4. “One-pot” coupling of three different partners.

Photophysical Properties

The absorption and emission spectra of the prototype compound **10a** in acetonitrile are presented in Figure 3 (solid lines). The absorption spectrum presents a vibrationally structured band with a maximum at 417 nm and a second peak in the UV region (250–270 nm).

Compound **10a** is strongly luminescent ($\Phi_{\text{em}} = 0.33$) with an emission band maximum at 494 nm in air-equilibrated acetonitrile. This can be attributed to fluorescence deactivation from the lowest singlet excited state (S_1) to the ground state (S_0) based on the short-lived emission intensity decay ($\tau = 2.2$ ns), which is not sensitive to the presence of dioxygen. In an ethanol rigid matrix at 77 K, the emission spectrum shows a better defined vibrational structure (dotted line in Figure 3) with a maximum at 463 nm and a longer lifetime ($\tau = 5.5$ ns). To investigate the effect of sol-

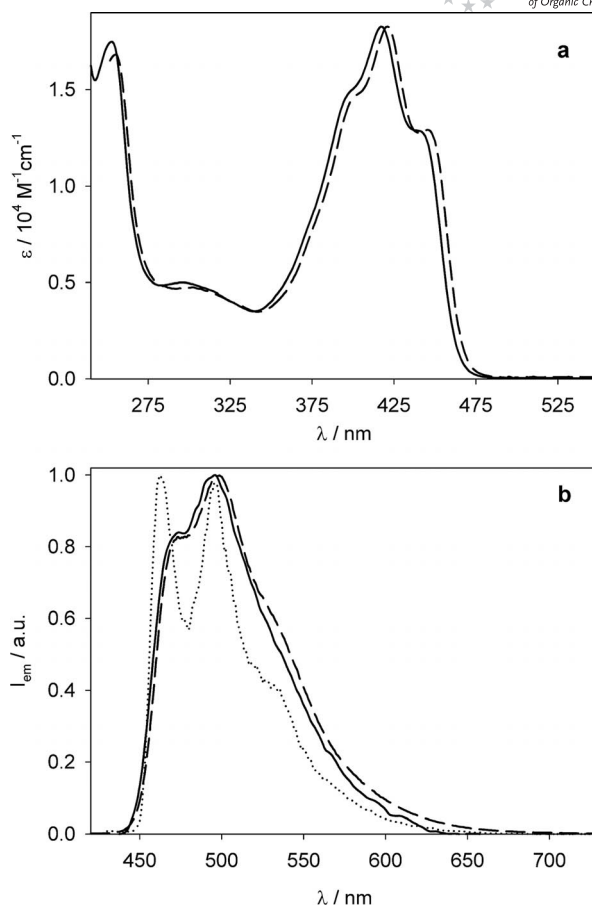


Figure 3. a) Absorption and b) emission spectra of compound **10a** in air-equilibrated solutions of acetonitrile (solid lines) or dichloromethane (dashed lines) at 298 K ($\lambda_{\text{ex}} = 420$ nm). The emission spectra were recorded in optically matched solutions at the excitation wavelength. For comparison purposes, the emission spectrum recorded in a rigid ethanol matrix at 77 K is also presented (dotted line).

vent polarity, a solution of **10a** in air-equilibrated dichloromethane was investigated (dashed lines in Figure 3). A small redshift of both the absorption and emission maxima is observed as well as substantial increases in the emission quantum yield ($\Phi_{\text{em}} = 0.62$) and lifetime ($\tau = 4.3$ ns). Based on these results, we decided to measure the absorption and emission spectra as well as the emission quantum yields of the other pentacyclic compounds in air-equilibrated dichloromethane solution, in which compound **10a** shows the best performances (Table 4).

From the results reported in Table 4, the following conclusions can be drawn. 1) Compounds **10a–c** show very similar photophysical properties and so it can be deduced that methyl substituents do not affect the optical features, as expected. 2) Appending a phenyl group to the B ring (**10e**) lowers the emission quantum yield. 3) Electron-donating substituents on both the lateral A and C rings in the *para* position (compounds **11a**, **11c** and **16c**) cause a strong decrease in the emission quantum yield, but this effect is not present by appending an electron-withdrawing substituent such as fluorine (**11b**). 4) If the electron-donating substitu-

Table 4. Photophysical data for the pentacyclic compounds in air-equilibrated dichloromethane at 298 K.

	Absorption		Emission	
	λ_{\max} [nm]	λ_{\max} [nm]	λ_{\max} [nm]	Φ_{em}
10a	423	497	0.62	
10b	424	505	0.71	
10c	421	500	0.67	
10d	424	511	0.71	
10e	425	510	0.20	
10f	425	510	0.01	
10g	426	515	0.09	
10h	429	520	0.02	
10i	427	510	0.05	
11a	430	518	0.11	
11b	420	498	0.63	
11c	468	597	0.08	
11d	424	504	0.64	
16a	429	516	0.04	
16b	470	620	0.03	
16c	465	609	0.03	
16d	422	498	0.78	
16e	438	518	0.54	
16f	440	520	0.56	

ent is in the *para* position but only on the C ring, the compounds are poorly luminescent (**16a** and **16b**), whereas they show strong luminescence if the same substituent is on the A ring (**16d** and **16e**). 5) Electron-donating substituents at the *meta* position of the lateral A and C rings do not affect the photophysical properties (**11d** and **16f**).

To rationalize the effects of the presence of electron-donating substituents, we carried out a detailed photophysical investigation on compounds **10a**, **11a**, **16a** and **16d** in air-equilibrated solutions of acetonitrile and dichloromethane at 298 K as well as in an ethanol rigid matrix at 77 K (Table 5). The electrochemical properties of these compounds were also studied in acetonitrile (see below).

Compound **16d** shows photophysical properties very similar to those reported for **10a** under all the investigated experimental conditions, which confirms that the presence of a methoxy substituent on the A ring does not affect the photophysical properties. Compound **11a** and **16a** exhibit a redshifted maximum of both the lowest-energy absorption band and fluorescence band. At 298 K in solution, their emission quantum yields and the S_1 lifetimes are considerably reduced, particularly in acetonitrile solution, whereas in the ethanol rigid matrix at 77 K, they have much longer

excited-state lifetimes. The emission quenching of **11a** and **16a** demonstrates that for these compounds there is an additional non-radiative decay competing with the radiative decay, which is prevented at 77 K. These results can be rationalized on the basis of the presence of a non-emitting charge-transfer (CT) state. Population of this state is possible at 298 K, whereas it is prevented at 77 K because the lack of solvent reorganization shifts the corresponding CT state to a higher energy. However, this hypothesis is not consistent with the electrochemical data reported below. For example, the energies of the CT state of both **10a** and **16a**, calculated on the basis of the first reduction and oxidation potentials (see Table 6), are very close to that of the S_1 excited state. Therefore no substantial difference between **10a** and **16a** is expected.

Based on the strong difference in the emission properties at 298 and 77 K, we decided to carefully investigate the emission as a function of temperature to determine whether the quenching mechanism is a thermally activated deactivation pathway. The lifetime of the luminescent excited state of **11a** in ethanol was recorded as a function of temperature in the range from 300 to 85 K (Figure 4). The S_1 lifetime and the fluorescence quantum yield are proportional, $\Phi = k_r\tau$, with k_r being the radiative rate constant, which is usually slightly sensitive to temperature. The lifetime is extremely short (ca. 0.5 ns) in the range 200–300 K and increases significantly close to the fluid-to-solid transition, reaching around 4.8 ns at 85 K. The emission maximum undergoes a blueshift from 513 to 480 nm on going from 300 to 85 K. The abrupt increase in lifetime and concomitant shift of the emission maximum suggest that the rigidity of the matrix influences the photophysical properties. These results are consistent with a rigidochromic effect: in a rigid matrix the solvent cannot reorganize around the excited state (which exhibits a different electronic distribution compared with the ground state) and creates a cage-like structure in which some non-radiative deactivations are slowed.^[14]

Because the rigidity of the matrix plays a crucial role in determining the luminescence of compound **11a**, we decided to investigate the luminescence properties of **11a** in a polymeric film at 298 K. The film was obtained by spin-coating a dichloromethane solution containing poly(methyl methacrylate) (PMMA) and **11a** (50:1, w/w). The film is highly emitting and exhibits an emission lifetime of more

Table 5. Emission data for compounds **10a**, **11a**, **16a** and **16d** in air-equilibrated dichloromethane and acetonitrile (in parentheses) at 298 K and in an ethanol rigid matrix at 77 K.

	Absorption at 298 K		Emission at 298 K			Emission at 77 K	
	λ_{\max} [nm]	ϵ [$10^4 \text{ M}^{-1} \text{ cm}^{-1}$]	λ_{\max} [nm]	Φ_{em}	τ [ns]	λ_{\max} [nm]	τ [ns]
10a	423 (417)	1.8 (1.8)	497 (494)	0.62 (0.33)	4.3 (2.2)	463	5.5
11a	430 (426)	1.8 (1.8)	518 (513)	0.11 (0.025)	0.7 (0.4)	480	4.8
16a	429 (425)	2.0 (2.0)	516 (519)	0.04 (0.009)	< 0.4 (<0.4)	484	4.5
16d	422 (419)	1.7 (1.7)	498 (495)	0.78 (0.66)	5.1 (4.7)	464	5.8

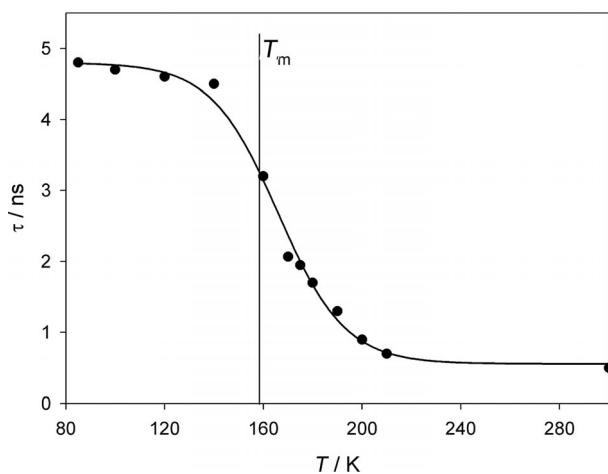


Figure 4. Temperature dependence of the emission lifetime of **11a** in air-equilibrated ethanol. T_m represents the melting point of the solvent.

than 2 ns, which confirms that rigidity is an important parameter. This result is very important in view of future applications in solid-state devices.

Electrochemical Properties

Compounds **10a**, **11a**, **16a** and **16d** were characterized electrochemically in acetonitrile with tetraethylammonium hexafluorophosphate (TEAPF₆) as supporting electrolyte (Table 6). The compounds were chosen to study the effect of the methoxy substituents on the pentacyclic moiety.

Table 6. Half-wave potentials ($E_{1/2}$ vs. SCE), unless otherwise noted, in acetonitrile/TEAPF₆ solution at 298 K.

	E_{ox} [V]	$E(1)_{red}$ [V]	$E(2)_{red}$ [V]
10a	+1.06 ^[a]	-1.52	-1.85 ^[a]
11a	+0.93 ^[a]	-1.61	-1.94 ^[a]
16a	+0.97 ^[a]	-1.56	-1.91 ^[a]
16d	+1.03 ^[a]	-1.58	-1.90 ^[a]

[a] Chemically irreversible process. Peak potential at 1 V/s.

All the investigated compounds show a chemically irreversible oxidation process (see, for example, peak A for **16a** in Figure 5). The product generated after oxidation (P) is reduced at around -0.09 V versus SCE (peak B, Figure 5), and this reduction is followed by a chemical reaction that is not reversible (Scheme 5).

Complete chemical reversibility was not attained by increasing the scan rate up to 10 V/s at 298 and 233 K. The experiment at 233 K was performed to reduce the rate of reaction (2) in Scheme 5.

In the cathodic region, a reversible process (peak I, Figure 5) is observed followed by one chemically irreversible process. The $E_{1/2}$ value of the first reduction process decreases in the order **10a** > **16a** > **16d** > **11a**, as expected by the presence of electron-donating methoxy substituents. An opposite trend is observed for the anodic peak potential of the oxidation process: if we assume that the rate of reaction (2) is the same for all the investigated compounds, the

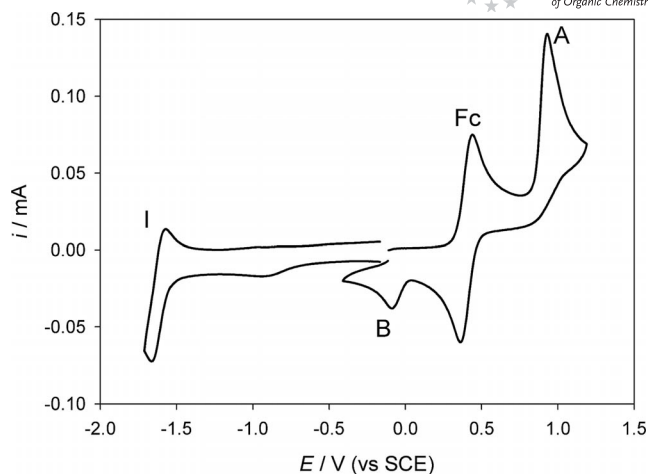


Figure 5. Cyclic voltammogram of **16a** in acetonitrile/TEAPF₆ solution at 298 K (scan rate: 1 V/s).



Scheme 5.

observed trend can again be rationalized on the basis of the effect of the methoxy substituent. The electrochemical data show slight changes in the reduction potentials of the investigated compounds, in agreement with the photophysical properties (Table 4). The energy of the luminescent excited state is slightly affected by the substituents.

Computational Studies

The data reported above show that in **16a** and **16d**, which differ in the position of the methoxy substituent, the energies of the luminescent excited state and the reduction potentials are only slightly different, whereas both the emission quantum yield and lifetime of the fluorescent excited state decrease strongly on going from **16d** to **16a**. These changes are likely due not to different electronic distributions of the π molecular orbitals (MOs) involved in the transition, but to a thermally activated non-radiative deactivation process, more favoured in **16a** than in **16d**.

To support this interpretation, density functional theory calculations were carried out on the neutral states of **10a**, **16a**, **16d** and **11a** by using the B3LYP functional^[15] and the standard 6-31G(d) basis set to compare the (gas-phase) energies and localization properties of the highest- and lowest-unoccupied MOs (HOMO and LUMO, respectively). Moreover, the energies of their singlet excited states were calculated by using the TD-B3LYP^[16] method. The adiabatic electron affinities (EA_{as}) were evaluated as the total energy difference between the neutral and anion ground states, each in its optimized geometry. Owing to the spa-

tially diffuse electron distributions of the anions,^[17] the EA_as were obtained by using the 6-31+G(d) basis set (which also includes s- and p-type diffuse functions at the non-hydrogen atoms). This computational method reproduced very accurately the (positive) EA_as measured in polyaromatic hydrocarbons.^[18] The results are reported in Table 7, together with the experimental absorption energies and reduction potentials for the sake of comparison.

Table 7. Calculated orbital energies, energies of the first singlet π - π^* transition and the adiabatic electron affinities. The experimental excitation energies and reduction potentials are also reported.

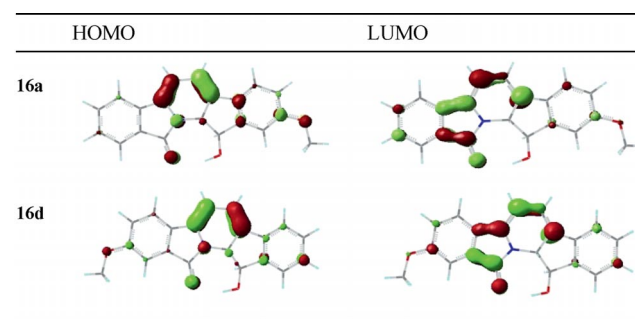
	B3LYP/6-31G(d)			Exp.		
	HOMO [eV]	LUMO [eV]	Abs. [nm]	EA _a ^[a] [eV]	Abs. [nm]	$E_{1/2}$ [eV]
10a	-5.290	-2.165	434.1	1.333 (1.436)	423	-1.52
11a	-4.956	-1.936	446.6	1.161 (1.269)	430	-1.61
16a	-5.067	-2.039	446.4	1.226 (1.330)	429	-1.56
16d	-5.164	-2.058	433.7	1.265 (1.366)	422	-1.58

[a] EA_as calculated with the 6-31+G(d) basis set. Values in parentheses include zero-point vibrational energy corrections.

According to the calculations, the O \cdots H hydrogen-bond distances [**10a**: 1.958 Å; **16a**: 1.942 Å; **16d**: 1.954 Å; **11a**: 1.943 Å; data obtained with the B3LYP/6-31+G(d) method] undergo small changes upon methoxy substitution and are only slightly shorter than that (2.00 Å) measured in **10b** in the solid state.^[8] The calculated MO energies show that each methoxy substitution causes a small destabilization of the HOMO and an almost equal destabilization of the LUMO. In agreement, the TD-B3LYP calculations predict quite similar HOMO–LUMO transition energies in the four compounds, the largest difference being <0.1 eV. The calculated absorption energies closely parallel the experimental counterparts measured in acetonitrile solution (see Table 6). The energies (not reported) of the second absorption band observed experimentally are also satisfactorily reproduced by the calculations. The HOMO and LUMO localization properties are predicted to be similar in the four compounds considered, in line with their relatively small localization on the methoxy groups. In particular, the representations determined by the B3LYP/6-31G(d) calculations for the HOMOs and LUMOs of **16a** and **16d** are given in Table 8.

The calculated EA_as are largely positive (Table 7) and close to that of pentacene,^[19] thus confirming the expectation that these polycyclic conjugated π systems are strong electron acceptors. The unsubstituted compound (**10a**) is predicted to possess the largest EA_a, but that of the disubstituted **11a** is only 0.2 eV smaller, the EA_as of **16a** and **16d** being intermediate and very close to each other. Note that the trend in EA values closely parallels that of the calculated LUMO energies of the neutral molecules and that of the reduction potentials measured in solution (see Table 7), although their variation along the series is even smaller.

Table 8. Representation of the HOMOs and LUMOs of compounds **16a** and **16d**, as deduced by B3LYP/6-31G(d) calculations.



Conclusions

New highly fluorescent pentacyclic derivatives containing the pyridoisindole subunit have been obtained in one or two steps from simple starting materials. The cross-coupling of one dihalopyridine and two (identical) boronic acids delivers the pentacyclic framework in generally good chemical yields. As a result of the flexibility of the reaction, different substituents were introduced at various positions of the pentacycles, thus allowing the preparation of a large number of fluorophores. Their photophysical properties demonstrate that the presence of electron-donating or -withdrawing substituents does not cause substantial changes in the absorption and emission maxima, but strongly influences the fluorescence quantum yield and the lifetime of the luminescent excited state. This result has been rationalized on the basis of a thermally activated non-radiative deactivation process. Indeed, a detailed investigation of a selected family of compounds has shown that the quenching mechanism active at room temperature in fluid solution is prevented at 77 K. Computational studies confirmed that the electronic distributions of the π molecular orbitals involved in the transition are very similar for the investigated compounds. Indeed, cyclic voltammetry shows a reversible reduction process and a chemically irreversible oxidation process at very similar potentials for the different pentacyclic compounds.

Experimental Section

General: All reactions were performed under argon in oven-dried glassware. THF and toluene were distilled from sodium/benzophenone and stored over sodium. All other solvents and reagents were used as received. TLC was performed on silica gel plates and visualized with a UV lamp (254 nm). Chromatography was performed on silica gel (70–230 mesh). Melting points were measured with a Totoli apparatus. ¹H and ¹³C NMR spectra were recorded with Bruker AC-200 or AC-250 Fourier-transform spectrometers by using an internal deuterium lock. Chemical shifts are quoted in parts per million (ppm) downfield of tetramethylsilane. Coupling constants (*J*) are quoted in Hz. Electronic impact mass spectra (EIMS) were recorded with a Shimadzu QP 2010 apparatus. High-resolution mass spectra were recorded with a Bruker micrOTOFQ spectrometer. Photophysical experiments were carried out in air-equilibrated acetonitrile or dichloromethane at 298 K or in an eth-

anol rigid matrix at 77 K. UV/Vis spectra were recorded with a Perkin–Elmer λ 650 spectrophotometer. Fluorescence spectra were recorded with a Varian Cary Eclipse spectrofluorimeter equipped with a Hamamatsu R928 phototube. Fluorescence quantum yields were measured following the method of Demas and Crosby^[20] (standard used: perylene in ethanol solution, $\Phi = 0.92$).^[21] Fluorescence lifetime measurements were performed with an Edinburgh FLS920 spectrofluorimeter equipped with a TCC900 card for data acquisition in time-correlated single-photon counting experiments (0.4 ns time resolution) with a LDH-P-C-405 pulsed diode laser. The estimated experimental errors are 2 nm for the band maximum, 5% for the molar absorption coefficient and the fluorescence lifetime and 15% for the fluorescence quantum yield. The electrochemical experiments were carried out in argon-purged acetonitrile at 298 and 233 K. Cyclic voltammetry (CV) was performed with a glassy carbon the working electrode (0.08 cm²), a Pt spiral counter electrode, and a silver wire was employed as a quasi-reference electrode (AgQRE). The potentials reported were referenced to SCE by measuring the AgQRE potential relative to ferrocene ($E_{1/2} = 0.39$ V vs. SCE for Fc^{+/0}). The concentrations of the compounds were approximately 1×10^{-3} M; 0.1 M tetraethylammonium hexafluorophosphate (TEAPF₆) was added as supporting electrolyte. Cyclic voltammograms were obtained at scan rates in the range 0.05–10 V s⁻¹. The estimated experimental error in the $E_{1/2}$ value is ± 10 mV.

General Procedure for the Preparation of Pentacycles 10: To a degassed solution of toluene (15 mL) containing [Pd(PPh₃)₄] (116 mg, 0.01 mmol) and 2,5-dihalopyridine **1**, **3** or **4** (1 mmol), degassed solutions of (2-formylphenyl)boronic acid (**6a**; 2.5 mmol) in methanol (2.5 mL) and Na₂CO₃ (5 mmol) in water (5 mL) were successively added. After heating for 12 h at 100 °C, the reaction mixture was cooled to room temperature, extracted with ethyl acetate (3 \times 20 mL) and dried with anhydrous magnesium sulfate (MgSO₄). After filtration through Celite and concentration, the residue was purified by chromatography on silica gel (cyclohexane/ethyl acetate) to give the desired compound.

13-(4-Formylphenyl)-7,8-dihydro-8-hydroxy-7H-indeno[1',2':4,5]pyrido[2,1-*a*]isoindol-5-one (10f): M.p. 127 °C. ¹H NMR (CDCl₃, 250 MHz): $\delta = 10.10$ (s, 1 H, CHO), 7.99 (d, $J = 5.0$ Hz, 2 H), 7.94 (d, $J = 5.0$ Hz, 1 H), 7.72–7.53 (m, 6 H), 7.36 (t, $J = 5.0$ Hz, 1 H), 7.08 (t, $J = 5.0$ Hz, 1 H), 6.78 (d, $J = 5.0$ Hz, 1 H), 6.25 (s, 1 H), 5.89 (s, 1 H, OH), 5.58 (d, $J = 4.0$ Hz, 1 H), 4.77 (d, $J = 4.0$ Hz, 1 H) ppm. ¹³C NMR (CDCl₃, 62.5 MHz): $\delta = 191.6, 169.5, 145.0, 144.3, 136.0, 134.9, 134.3, 132.3, 132.0, 130.4, 130.0, 129.8, 129.1, 128.3, 127.8, 125.1, 123.6, 123.5, 120.5, 106.8, 77.7, 66.7$ ppm. HRMS: calcd. for C₂₆H₁₇NO₃ 391.1215 [M + Na]⁺; found 414.1112.

7,8-Dihydro-8-hydroxy-13-(4-methylthiophenyl)-7H-indeno[1',2':4,5]pyrido[2,1-*a*]isoindol-5-one (10g): M.p. 109 °C. ¹H NMR (CDCl₃, 200 MHz): $\delta = 7.94$ (d, $J = 6.0$ Hz, 1 H), 7.71–7.50 (m, 5 H), 7.34 (s, 4 H), 7.10 (t, $J = 8.0$ Hz, 1 H), 6.91 (d, $J = 8.0$ Hz, 1 H), 6.25 (s, 1 H, H), 5.93 (s, 1 H, OH), 5.55 (d, $J = 6.0$ Hz, 1 H), 4.75 (d, $J = 6.0$ Hz, 1 H), 2.56 (s, 3 H, SMe) ppm. ¹³C NMR (CDCl₃, 50 MHz): $\delta = 169.5, 143.9, 138.7, 135.4, 135.1, 134.9, 133.8, 132.1, 131.3, 129.6, 129.5, 128.7, 1284, 128.3, 128.2, 126.6, 124.9, 123.6, 123.5, 120.4, 108.1, 66.7, 15.6$ ppm. HRMS: calcd. for C₂₆H₁₉NO₂S 409.1142 [M + Na]⁺; found 432.1029.

13-(4-Dimethylaminophenyl)-7,8-dihydro-8-hydroxy-7H-indeno[1',2':4,5]pyrido[2,1-*a*]isoindol-5-one (10h): M.p. 201 °C. ¹H NMR (CDCl₃, 200 MHz): $\delta = 7.92$ (d, $J = 6.0$ Hz, 1 H), 7.67–7.48 (m, 4 H), 7.31 (m, 3 H), 7.08 (m, 2 H), 6.80 (d, $J = 8.0$ Hz, 2 H), 6.31 (s, 1 H), 5.97 (s, 1 H), 5.55 (d, $J = 6.0$ Hz, 1 H), 4.76 (d, $J = 6.0$ Hz,

1 H), 3.04 (s, 6 H, NMe₂) ppm. ¹³C NMR (CDCl₃, 50 MHz): $\delta = 169.5, 150.2, 143.7, 135.9, 135.0, 133.5, 132.0, 130.5, 129.3, 129.2, 129.1, 129.0, 128.3, 128.1, 126.1, 124.7, 123.6, 123.4, 120.4, 112.4, 109.1, 66.7, 40.5$ ppm. HRMS: calcd. for C₂₇H₂₂N₂O₂ 406.1691 [MH]⁺; found 407.1770.

7,8-Dihydro-8-hydroxy-13-(4-methoxyphenyl)-7H-indeno[1',2':4,5]pyrido[2,1-*a*]isoindol-5-one (10i): M.p. 184 °C. ¹H NMR (CDCl₃, 200 MHz): $\delta = 7.92$ (d, $J = 6.0$ Hz, 1 H), 7.75–7.48 (m, 4 H), 7.27–7.37 (m, 3 H), 7.09 (t, $J = 7.6$ Hz, 1 H), 7.00 (d, $J = 8.8$ Hz, 2 H), 6.91 (d, $J = 7.8$ Hz, 1 H), 6.27 (d, $J = 1.4$ Hz, 1 H), 5.94 (d, $J = 1.4$ Hz, 1 H), 5.55 (d, $J = 6.0$ Hz, 1 H), 4.76 (d, $J = 6.0$ Hz, 1 H), 3.89 (s, 3 H, OMe) ppm. ¹³C NMR (CDCl₃, 62.5 MHz): $\delta = 169.5, 159.5, 143.9, 135.6, 135.0, 133.7, 132.1, 131.2, 130.8, 129.5, 129.4, 128.8, 128.3, 128.2, 124.9, 123.6, 123.5, 120.4, 114.4, 108.5, 77.9, 66.7, 55.3$ ppm. HRMS: calcd. for C₂₆H₁₉NO₃ 393.1373 [M + Na]⁺; found 416.1270.

General Procedure for the Preparation of Pentacycles 16: Degassed solutions of boronic acid **6** (0.75 mmol) in methanol (1 mL) and Na₂CO₃ (110 mg, 1 mmol) in water (1 mL) were successively added to a degassed solution of toluene (2 mL) containing [Pd(PPh₃)₄] (29 mg, 0.025 mmol), NaBr (only with chlorinated substrates **12**; 50 mg, 0.5 mmol) and pyridylbenzaldehyde **12** or **13** (0.5 mmol). After heating for 12 h at 100 °C, the reaction mixture was cooled to room temperature, extracted with ethyl acetate and dried with MgSO₄. After concentration, the residue was purified by chromatography on silica gel (cyclohexane/ethyl acetate) to give the desired compounds.

7,8-Dihydro-8-hydroxy-10-methoxy-7H-indeno[1',2':4,5]pyrido[2,1-*a*]isoindol-5-one (16a): M.p. 152 °C. ¹H NMR (CDCl₃, 200 MHz): $\delta = 7.83$ (d, $J = 7.0$ Hz, 1 H), 7.65–7.30 (m, 4 H), 7.12 (s, 1 H), 6.88 (dd, $J = 2.0, 8.0$ Hz, 1 H), 6.32 (dd, $J = 2.0, 6.0$ Hz, 1 H), 6.23 (d, $J = 6.0$ Hz, 1 H), 5.83 (s, 1 H, OH), 5.35 (d, $J = 6.0$ Hz, 1 H), 4.60 (dd, $J = 2.0, 6.0$ Hz, 1 H), 3.84 (s, 3 H, OMe) ppm. ¹³C NMR (CDCl₃, 50 MHz): $\delta = 169.5, 161.6, 145.2, 136.7, 135.0, 132.9, 131.8, 128.8, 128.6, 127.7, 123.1, 122.2, 120.1, 116.8, 110.5, 108.4, 104.2, 78.1, 66.0, 55.5$ ppm. HRMS: calcd. for C₂₀H₁₅NO₃ 317.1047 [M + Na]⁺; found 340.0944.

10-(Dimethylamino)-7,8-dihydro-8-hydroxy-7H-indeno[1',2':4,5]pyrido[2,1-*a*]isoindol-5-one (16b): M.p. 193 °C. ¹H NMR (CDCl₃, 200 MHz): $\delta = 7.86$ (d, $J = 7.0$ Hz, 1 H), 7.70–7.35 (m, 4 H), 6.90 (s, 1 H), 6.70 (d, $J = 8.0$ Hz, 1 H), 6.28 (s, 2 H), 5.94 (s, 1 H, OH), 5.37 (d, $J = 6.0$ Hz, 1 H), 4.63 (d, $J = 6.0$ Hz, 1 H), 3.03 (s, 6 H, NMe₂) ppm. ¹³C NMR (CDCl₃, 50 MHz): $\delta = 169.5, 152.1, 145.2, 137.8, 135.1, 131.9, 131.7, 128.4, 127.6, 124.0, 123.1, 122.2, 119.9, 113.1, 108.3, 107.1, 105.1, 78.2, 66.1, 40.5$ ppm. HRMS: calcd. for C₂₁H₁₈N₂O₂ 330.1368 [M + Na]⁺; found 353.1260.

10-(Dimethylamino)-7,8-dihydro-8-hydroxy-3-methoxy-7H-indeno[1',2':4,5]pyrido[2,1-*a*]isoindol-5-one (16c): M.p. 144 °C. ¹H NMR (CDCl₃, 200 MHz): $\delta = 7.56$ (d, $J = 8.5$ Hz, 1 H), 7.39–7.31 (m, 2 H), 7.12 (d, $J = 8.5$ Hz, 1 H), 6.92 (s, 1 H), 6.72 (d, $J = 8.0$ Hz, 1 H), 6.27 (d, $J = 6.0$ Hz, 1 H), 6.17 (d, $J = 6.5$ Hz, 1 H), 5.91 (s, 1 H, OH), 5.36 (d, $J = 5.5$ Hz, 1 H), 4.61 (d, $J = 4.5$ Hz, 1 H), 3.89 (s, 3 H, OMe), 3.04 (s, 6 H, NMe₂) ppm. ¹³C NMR (CDCl₃, 50 MHz): $\delta = 169.5, 160.5, 152.0, 145.1, 136.9, 131.9, 129.3, 128.2, 124.4, 122.1, 121.3, 120.6, 113.3, 108.5, 107.3, 105.4, 103.8, 78.3, 66.3, 55.7, 40.6$ ppm. HRMS: calcd. for C₂₂H₂₀N₂O₃ 360.1481 [M + H]⁺; found 361.1561.

7,8-Dihydro-8-hydroxy-3-methoxy-7H-indeno[1',2':4,5]pyrido[2,1-*a*]isoindol-5-one (16d): M.p. 209 °C. ¹H NMR (CDCl₃, 200 MHz): $\delta = 7.58$ (m, 2 H), 7.48 (dd, $J = 1.5, 4.0$ Hz, 1 H), 7.40–7.31 (m, 3 H), 7.17 (dd, $J = 1.5, 4.0$ Hz, 1 H), 6.52 (dd, $J = 1.5, 4.0$ Hz, 1 H),

6.19 (d, $J = 4.0$ Hz, 1 H), 5.73 (s, 1 H, OH), 5.45 (d, $J = 4.0$ Hz, 1 H), 4.68 (dd, $J = 1.5, 3.0$ Hz, 1 H), 3.84 (s, 3 H, OMe) ppm. ^{13}C NMR (CDCl_3 , 50 MHz): $\delta = 169.6, 161.0, 143.1, 136.1, 133.9, 129.7, 129.6, 128.8, 127.9, 125.1, 121.6, 120.9, 120.6, 112.9, 105.7, 102.4, 78.4, 66.1, 55.8$ ppm. HRMS: calcd. for $\text{C}_{20}\text{H}_{15}\text{NO}_3$ 317.1053 [M + Na] $^+$; found 340.0950.

3-(Dimethylamino)-7,8-dihydro-8-hydroxy-7H-indeno[1',2':4,5]pyrido[2,1-a]isoindol-5-one (16e): M.p. 195 °C. ^1H NMR (CDCl_3 , 200 MHz): $\delta = 7.62\text{--}7.33$ (m, 5 H), 7.07 (s, 1 H), 6.88 (dd, $J = 2.0, 8.0$ Hz, 1 H), 6.47 (dd, $J = 3.0, 6.0$ Hz, 1 H), 6.04 (d, $J = 6.0$ Hz, 1 H), 5.83 (s, 1 H, OH), 5.40 (d, $J = 6.0$ Hz, 1 H), 4.62 (dd, $J = 2.5, 5.5$ Hz, 1 H), 3.04 (s, 6 H, NMe_2) ppm. ^{13}C NMR (CDCl_3 , 50 MHz): $\delta = 170.4, 151.4, 142.9, 136.3, 134.7, 134.6, 129.6, 129.2, 128.6, 125.0, 122.8, 121.4, 120.7, 116.0, 113.3, 104.8, 100.4, 78.5, 66.1, 40.5$ ppm. HRMS: calcd. for $\text{C}_{21}\text{H}_{18}\text{N}_2\text{O}_2$ 330.1365 [M + H] $^+$; found 331.1445.

10-(Dimethylamino)-7,8-dihydro-8-hydroxy-3-methoxy-7H-indeno[1',2':4,5]pyrido[2,1-a]isoindol-5-one (16f): M.p. 196 °C. ^1H NMR (CDCl_3 , 200 MHz): $\delta = 7.51$ (s, 2 H), 7.48 (d, $J = 2.5$ Hz, 1 H), 6.95–6.87 (m, 3 H), 6.51 (d, $J = 6.0$ Hz, 1 H), 6.04 (d, $J = 6.0$ Hz, 1 H), 5.74 (s, 1 H, OH), 5.36 (d, $J = 5.5$ Hz, 1 H), 4.61 (dd, $J = 3.0, 5.0$ Hz, 1 H), 3.84 (s, 3 H, OMe), 3.06 (s, 6 H, NMe_2) ppm. ^{13}C NMR (CDCl_3 , 50 MHz): $\delta = 170.4, 160.4, 151.4, 137.7, 135.5, 134.7, 134.6, 129.7, 126.0, 122.8, 121.4, 116.4, 116.0, 113.3, 104.9, 104.7, 100.3, 78.0, 66.4, 55.5, 40.6$ ppm. HRMS: calcd. for $\text{C}_{22}\text{H}_{20}\text{N}_2\text{O}_3$ 360.1479 [M + Na] $^+$; found 383.1376.

Supporting Information (see footnote on the first page of this article): Experimental procedures and analytical data for pyridines **4**, boronic acids **8** and pyridylbenzaldehydes **12** and **13**, ^1H and ^{13}C NMR spectra for all new compounds.

Acknowledgments

This work has been supported by the Centre National de la Recherche Scientifique (CNRS), the Université de Lorraine, by the Ministère de l'Enseignement Supérieur et de la Recherche (grant to Z. C.), the Ministero dell'Università e della Ricerca (MIUR) (PRIN 20085ZXFEE, PRIN 2009SLKFEX and FIRB RBAP11C58Y) and by MAE DGPC (Dendrimeri come nuovi materiali per celle solari ecocompatibili).

[1] a) M. Pawlicki, H. A. Collins, R. G. Denning, H. L. Anderson, *Angew. Chem.* **2009**, *121*, 3292–3316; *Angew. Chem. Int. Ed.* **2009**, *48*, 3244–3266; b) J. Kalinowski, *Opt. Mater.* **2008**, *30*, 792–799.

- [2] a) K. E. Sapsford, L. Berti, I. L. Medintz, *Angew. Chem.* **2006**, *118*, 4676–4704; *Angew. Chem. Int. Ed.* **2006**, *45*, 4562–4588; b) M. S. T. Gonçalves, *Chem. Rev.* **2009**, *109*, 190–212; c) L. D. Davis, R. T. Raines, *ACS Chem. Biol.* **2008**, *3*, 142–155.
- [3] T. S. A. Heugebaert, B. I. Roman, C. V. Stevens, *Chem. Soc. Rev.* **2012**, *41*, 5626–5640.
- [4] Y. Cheng, B. Ma, F. Wudl, *J. Mater. Chem.* **1999**, *9*, 2183–2188.
- [5] a) T. Mitsumori, M. Bendikov, O. Dautel, F. Wudl, T. Shioya, H. Sato, Y. Sato, *J. Am. Chem. Soc.* **2004**, *126*, 16793–16803; b) Y.-M. Chen, G. Grampp, N. Leesakul, H.-W. Hu, J.-H. Xu, *Eur. J. Org. Chem.* **2007**, 3718–3726.
- [6] a) J. Wan, C.-J. Zheng, M.-K. Fung, X.-K. Liu, C.-S. Lee, X.-H. Zhang, *J. Mater. Chem.* **2012**, *22*, 4502–4510; b) B. Liu, Z. Wang, N. Wu, M. Li, J. You, J. Lan, *Chem. Eur. J.* **2012**, *18*, 1559–1603; c) E. Kim, M. Koh, B. J. Lim, S. B. Park, *J. Am. Chem. Soc.* **2011**, *133*, 6642–6649; d) P. J. Aittala, O. Cramariuc, T. I. Hukka, M. Vasilescu, R. Bandula, H. Lemmetyinen, *J. Phys. Chem. A* **2010**, *114*, 7094–7101; e) M. Aginagalde, Y. Vara, A. Arrieta, R. Zangi, V. L. Cebolla, A. Delgado-Camon, F. P. Cossio, *J. Org. Chem.* **2010**, *75*, 2776–2784.
- [7] V. Mamane, Y. Fort, *Tetrahedron Lett.* **2006**, *47*, 2337–2340.
- [8] Z. Chamas, O. Dietz, E. Aubert, Y. Fort, V. Mamane, *Org. Biomol. Chem.* **2010**, *8*, 4815–4818.
- [9] F. Cottet, M. Schlosser, *Tetrahedron* **2004**, *60*, 11869–11874.
- [10] For the importance of temperature in the *ortho*-lithiation of **3**, see: M. Abboud, V. Manane, E. Aubert, C. Lecomte, Y. Fort, *J. Org. Chem.* **2010**, *75*, 3224–3231.
- [11] a) For **6b**, see: S. J. Kumar, *J. Chem. Soc. Perkin Trans. 1* **2001**, 1018–1032; b) for **6c**, see: S. Lozano Yeste, M. E. Powell, S. D. Bull, T. D. James, *J. Org. Chem.* **2009**, *74*, 427–430; c) for **6d**, see ref.^[8]
- [12] D. L. Comins, J. D. Brown, *J. Org. Chem.* **1984**, *49*, 1078–1083.
- [13] N. Kudo, M. Perseghini, G. C. Fu, *Angew. Chem.* **2006**, *118*, 1304–1306; *Angew. Chem. Int. Ed.* **2006**, *45*, 1282–1284.
- [14] M. Wrighton, D. L. Morse, *J. Am. Chem. Soc.* **1974**, *96*, 998–1003.
- [15] A. D. Becke, *J. Chem. Phys.* **1993**, *98*, 5648–5652.
- [16] R. E. Stratmann, G. E. Scuseria, M. J. J. Frisch, *Chem. Phys.* **1998**, *109*, 8218–8224.
- [17] T. H. Dunning, Jr., K. A. Peterson, D. E. Woon in *Basis Sets: Correlation Consistent Sets in the Encyclopedia of Computational Chemistry* (Ed.: P. v. R. Schleyer), Wiley, Chichester, UK, **1998**.
- [18] A. Modelli, L. Mussoni, D. Fabbri, *J. Phys. Chem. A* **2006**, *110*, 6482–6486.
- [19] L. Crocker, T. Wang, P. Kebarle, *J. Am. Chem. Soc.* **1993**, *115*, 7818–7822.
- [20] J. N. Demas, G. A. Crosby, *J. Phys. Chem.* **1971**, *75*, 991–1024.
- [21] M. Montalti, A. Credi, L. Prodi, M. T. Gandolfi, in: *Handbook of Photochemistry*, 3rd ed., Taylor & Francis Group, New York, **1996**.

Received: November 22, 2012
Published Online: March 13, 2013